

Algorithm for 2-Dimensional Super-Resolution Optical Inspection for Semiconductor Defects by Using Standing Wave Illumination

Ryota Kudo¹, Shin Usuki², Satoru Takahashi¹ and Kiyoshi Takamasu¹

¹ Department of Precision Engineering, The University of Tokyo, Faculty of Engineering Bldg.14, 7-3-1 Hongo, Bunkyo-ku, Tokyo, JAPAN

² Division of Global Research Leaders, Shizuoka University, 3-5-1 Johoku, Naka-ku, Hamamatsu, JAPAN

Corresponding Author / E-mail: honc@nanolab.t.u-tokyo.ac.jp, TEL: +81-3-5841-6472, FAX: +81-3-5841-6472,

KEYWORDS : standing wave illumination, image reconstruction, super-resolution

Semiconductor design rules and process windows continue to shrink, so we face many challenges in developing new processes such as less 100nm design rule and 300mm wafer. The challenges have become more difficult and the next generation defect inspection is urgently demanded. The optics and electron beam have been mainly used for detection of the critical defects, but both technologies have disadvantages. The optical inspection is generally not enough sensitive for defects at 100nm geometries and below, while the SEM inspection has low throughput because it takes long time in scanning 300mm. In order to find a solution to these problems, we proposed the novel optical inspection method for the critical defects on the semiconductor wafer. Proposed method is as described below. The sample is illuminated by standing wave, and standing wave illumination is shifted multiple times. Obtained multiple scattered light images are post-processed by computer. Thus, high frequency information of standing wave illumination and the effect of deconvolution are reflected in the solution, high resolution beyond Rayleigh limit is achieved. Until now, one dimensional resolution which is beyond Rayleigh limit is theoretically studied and experimentally brought to realization. For applying proposed method to sample which has two dimensional structure, two dimensional modulated light information is needed. So, we have proposed a method making standing wave shift in multiple directions, and carrying out super-resolution in each shifting direction. We construct the algorithm that can use multidirectional standing wave shift and achieve 2-D super-resolution. We carried out fundamental verification of this method. As a result, it is confirmed that multidirectional standing wave illumination shift enables resolving two dimensional structure with accurate shape which can't be resolved by normal imaging system.

Manuscript received: July 15, 2009 / Accepted: August 15, 2009

NOMENCLATURE

1-D = one dimension/two dimensional
 2-D = two dimension/two dimensional
 SWI = standing wave illumination
 PSF = point spread function

1. Introduction

According to the ITRS roadmap [1], a next-generation semiconductor defect inspection system is urgently demanded, and the challenges for defect detection increase exponentially with shrinking design, such as sub-100-nm nodes. One of the key areas where improvement is needed is defect detection of semiconductor wafers [2]. Defects in the wafers include random defects like killer particles, clustered defects, scratch defects and so on. These defects deteriorate electrical chip performance and process yield in the semiconductor manufacturing process. Especially, improved inspection of patterned wafers is a necessity for the next generation of semiconductors.

Optical methods and electron beams are conventionally used for semiconductor wafer inspection [3]. However, with the continuous miniaturization of interconnects, optical inspection becomes less useful because of its diffraction limit. On the other hand, electron beams lack utility for wider wafer inspection because of their low throughput property. We think optical inspection has greater potential than SEM inspection for inspection because optical inspection is non-destructive and has high throughput. So, we focused our attention on optical inspection. In optical patterned wafer inspection, resolution and defect detection beyond the Rayleigh limit are now required due to the acceleration of pattern miniaturization and development of advanced semiconductor devices [4].

One of the solutions to challenges in semiconductor optical inspection is the use of shorter wavelengths, which has been studied as a countermeasure against device miniaturization. However, as the shortening of wavelength is too limited to keep up with the challenges, we have developed a super-resolution inspection technique. Namely, when a pattern is miniaturized and made dense, light reflected from the wafer becomes weak, and the captured image becomes dark with low contrast; hence, a high-sensitivity method that can obtain a lot of optical information must be

developed [5]. Our super-resolution inspection technique combines a standing wave illumination shift method with dark-field imaging technology to deliver optimal sensitivity for critical defect detection at sub-100-nm nodes and beyond, without compromising throughput [6] [7]. The standing wave illumination shift method enables the optical resolution of patterns that the conventional method cannot achieve. Nano-scale shifts of illumination and super-resolution post-processing are keys to achieving the resolution enhancement and higher sensitivity for defect detection. In this report, to apply our super-resolution technique to 2-D structure, we improve the algorithm. The algorithm that save computational complexity and can use 2-D structured illumination is constructed. And with this algorithm, 2-D super-resolution is achieved. Then, we verify the resolution characteristics by computer simulation based on Fourier optics. And, it is confirmed that super-resolution multidirectional SWI shift can ease the dependency of direction and obtain correctly shifted 2-D reconstructed image.

2. Super-resolution by using SWI shift based on iterative reconstruct calculation

A schematic diagram of the standing wave illumination shift and the scattered light modulation is shown in Figure 1. The standing wave illumination is generated by 2-beam interference. The standing wave illumination is scattered by the sample surface, and the scattered light is focused on the CCD imaging surface through the imaging lens. The standing wave is shifted on a nanoscale by the phase difference between the 2 beams in the illumination (Fig.1 (a)). Then, the scattered light is modulated by the shift of the standing wave illumination (Fig.1 (b)). A super-resolution image of scattering efficiency can be iteratively calculated from multiple images by the super-resolution image reconstruction algorithm.

Fig.2 shows the schematics of 1-D super resolution. When two point samples to be observed are close enough (shown as two blue dots), the two points cannot be distinguished in the observed image. Then, the sample is illuminated by the standing wave, and multiple modulated scattered light images are obtained. These obtained images are post-processed, and then the two point samples are clearly resolved as shown in the lower right image. Thus, a super resolution is achieved.

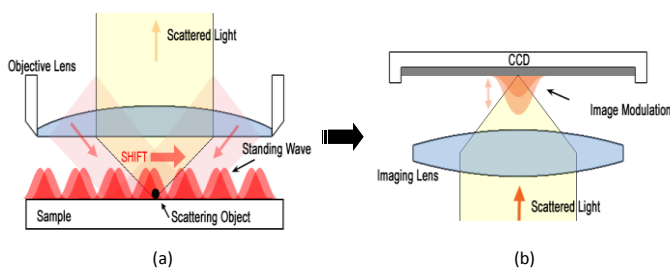


Fig. 1 Schematic diagram of the standing wave illumination shift and the scattered light modulation

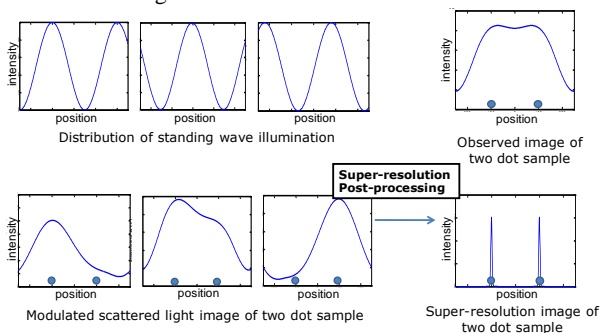


Fig. 2 The schematics of super-resolution (1-D)

The resolution improvement of proposed method consists of two

effects, band expansion and iterative reconstruction. The resolution with effect of band expansion: R_{SLI} can be estimated by following expression. (1)

$$R_{SLI} = \frac{1.22}{f_c + f_m} = \frac{1.22}{\frac{2NA}{\lambda} + \frac{1}{T}}, \quad (1)$$

where, f_c is cutoff frequency, f_m is frequency of SWI, λ is wavelength, and T is pitch of SWI.

The proposal method is not a technique that uses only the expansion of the frequency space band [8] [9], but also the effects by iterative reconstruct calculation within a real space. It is verified that resolution of 100 nm scale is possible under the random noise mixing environment of 20 percent in the 1-D super-resolution with band expansion and iterative reconstruct effect, however it is difficult to formulate this iterative reconstruct effect.

3. Algorithm for 2-D super-resolution

A block diagram of the 2-D super-resolution post-processing is shown in the Fig.3 and Fig.4. First, the sample is illuminated with standing wave illumination, and multiple images are experimentally observed by the standing wave shift. Then, using assumed sample which is firstly set as constant sample, calculated images are computationally obtained based on Fourier optics. The error between the observed images and the calculated images is approximately fed back to the assumed sample to obtain a reconstructed sample. The image reconstruction is iteratively calculated with successive approximation until the error converges. The nanoshifts of standing wave illumination that are modulated at about a half-wavelength scale include high-frequency spatial information, and this causes change to the scattered light images. We expect to achieve super resolution by feeding back the errors in scattered light images into sample distribution and reconstructing the sample distribution with successive approximation. As shown in Fig.4, multidirectional SWI shift is needed for getting 2-D modulated information of scattered light.

Generally speaking, to process deconvolution within a real space and to do 2-D reconstruction accurately, there is a problem of needing the matrix of an unrealistic huge size. In super-resolution post-process, error distribution matrix is going to be too big. To deal with this problem, the algorithm has been improved so that all information on 2-D blur of the point spread function is not used but the information of center one point with the largest contribution is only used. Though PSF information is simplified in the distribution of the error, blur information on 2-D PSF is reflected when images are calculated based on Fourier optics. So, it settles to a correct solution by the iterative loop.

As results of this improvement, saving of the computational complexity was achieved, and the 2-D reconstruction became possible. And it became possible to use the illumination which has 2-D distribution (e.g. Fig.5 (c), (d)) for super-resolution.

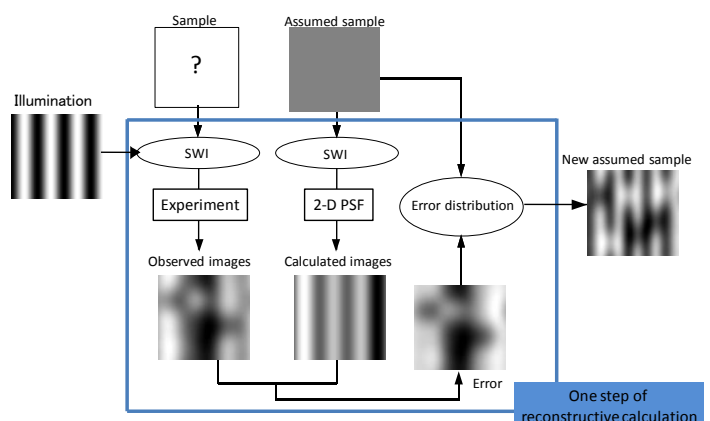


Fig. 3 One step of 2-D super-resolution reconstructive calculation

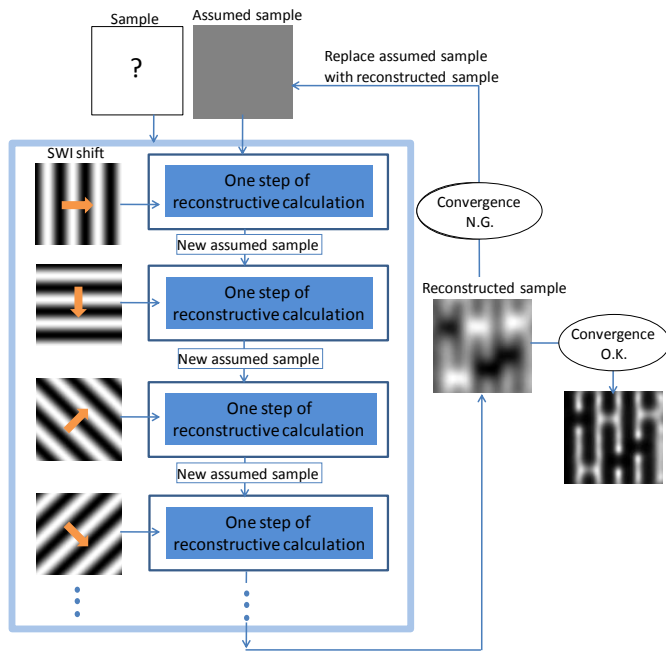


Fig. 4 The whole algorithm of 2-D super-resolution reconstructive calculation

4. 2-D Super-Resolution Simulation (Comparison Between 2 Direction and 4 Direction SWI Shift)

To verify the fundamental resolution characteristics of the 2-D super-resolution algorithm mentioned before, several computer simulations based on Fourier optics are carried out. In these simulations, we employ concentric circles sample for qualitative evaluation (4.1) and periodical grating sample for quantitative evaluation (4.2). The 2-D super-resolution simulation conditions are defined in Table 1. In this report, four directions of SWI which is generated by 2-beam interference (Fig.5) are taken in consideration as multidirectional SWI. We mainly focus on the difference between 2-direction SWI shift super-resolution and 4-direction SWI shift super-resolution.

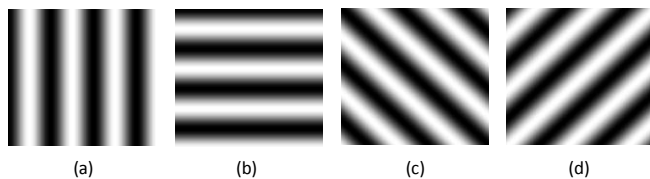


Fig. 5 Four directions of SWI

Table 1 Simulation conditions

Wavelength of source	488nm
Pitch of structured light illumination	300nm
NA of objective	0.95
Rayleigh limit	313nm
Resolution estimated by effect of band expansion	169nm
Shift times in each directions	10
Shift step size	30nm

4.1 Qualitative evaluation of reconstructive shape with concentric circles sample

First, we attempted super resolution on a concentric circles sample to investigate the dependency in direction of 2D super-resolution qualitatively. Here, an assumed sample, which consists of an outer ring being concentric with a center circle, is set as shown in Fig.6 (a). The radius of outer ring is 168nm, and the

radius of center circle is 37nm. Fig.6 (b) is the normal microscopic image of uniform illumination: a bandwidth-limited image by NA. It is confirmed that the structure of the sample is not resolved in Fig.6 (b). Examples of changing images by standing wave illumination shift are shown in Fig.6 (c)-(j). The smaller figures inset at the upper left corners show the directions of SWI. The larger figures show the sample images illuminated by the SWI. As these figures show, SWI shifts in 4 directions and for each direction of standing wave illumination, modulated images are obtained.

Using obtained images, 2-D super-resolution post-processing is carried out. Iteration time was set as 1000 times enough to converge. Fig.6 (k) is the super-resolution image by 2-direction SWI shift. Two SWI distributions (Fig.5 (a), (b)) are used for super-resolution. The reconstruction result almost corresponds to the distribution of the sample, though round sample becomes like the quadrangle. The dependency by the angle was confirmed. In this case, it comes to show the band expansion described in frequency space by Fig.7 (a). Information on the band shown with blue center circle is only included in the obtained image before the expansion of the band (Fig.6 (b)). The bands shown by black circles are expanded by SWI. There is direction dependency of band expansion. And this dependency causes inaccurate result of super-resolution.

On the other hand, in super-resolution image by 4-direction SWI shift (Fig.6 (l)), the result that shape is more correctly reconstructed was obtained. It was confirmed that the dependency by the direction was more eased by 4-direction SWI shift than 2-direction SWI shift. This is because following reason. If four SWI distributions (Fig.5 (a)-(d)) used, band expansion becomes like Fig.7 (b). It is shown that the direction dependency is reduced.

The multidirectional illumination shift such as 4-direction SWI shift is preferable to achieve 2-D super-resolution effectively.

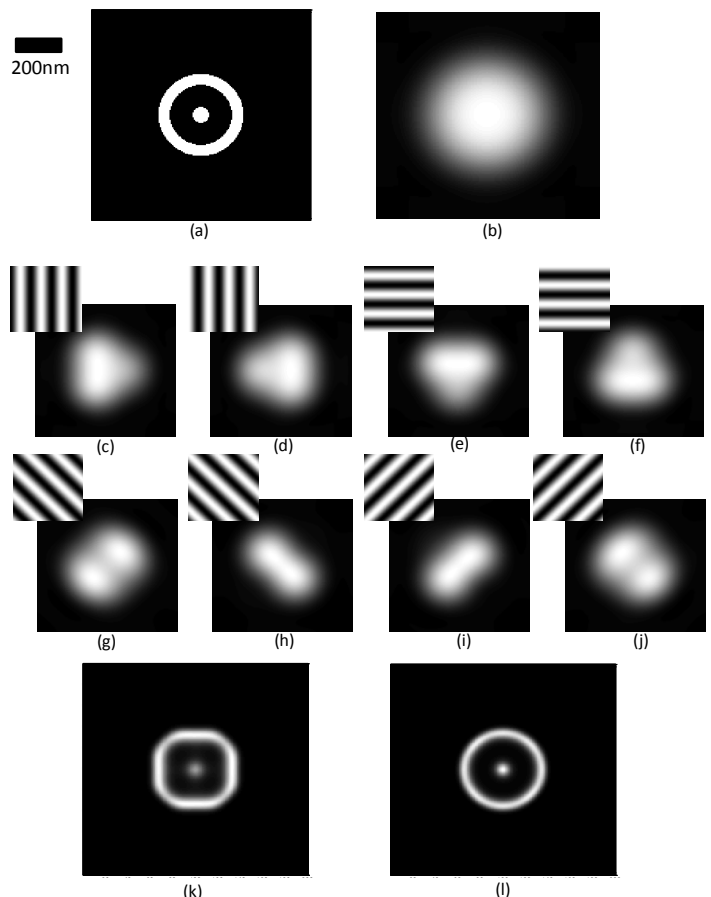


Fig. 6 Simulation for qualitative evaluation of dependency in direction (a) Sample (b) Sample image under uniform illumination (c)-(j) Examples of modulated light images by SWI (k) Super-resolution image by 2-direction SWI shift (l) Super-resolution image by 4-direction SWI shift

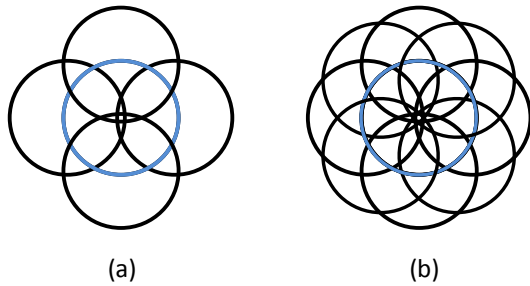


Fig. 7 Band expansion described in frequency space
(a) 2-direction SWI shift (b) 4-direction SWI shift

4.2 Quantitative evaluation of reconstructive shape with periodical grating samples

In this section, 2-D super-resolution simulation is carried out on other samples. It was tried to evaluate the direction dependency quantitatively by inclining the periodical grating sample with the distribution of the sine wave (Fig.8 (a)), and processing a super-resolution at each angle. A periodical grating sample which has 150nm pitch was inclined from 0 to 90 degrees at intervals of five degrees, and the super-resolution post-process was given. The simulation conditions are as defined in Table 1. Iteration time was set as 200 times enough to see the basic resolving characteristics.

The three cases are shown in Fig.8 as examples (Fig.8 (A): inclined angle 10 degrees, Fig.8 (B): inclined angle 25 degrees, Fig.8 (C): inclined angle 45 degrees). Fig.8 (a) show the sample distributions. 2-direction SWI shift super-resolution images are shown in Fig.8 (b), and in Fig.8 (c), 4-direction SWI shift super-resolution images are shown. Right images of Fig.8 (b), (c) are profile of intensity distribution along dotted line in left images. Both of super-resolution images (Fig.8 (A)(a), Fig.8 (A)(b)) clearly resolve structure of the sample. Under the condition of Rayleigh limit 313nm,

and resolution estimated by effect of band expansion 169nm calculated by expression (1), 150nm pitch of sample is resolved. If there is only effect of band expansion, the resolution of the Rayleigh limit level should be obtained with case of 169nm pitch structure, because resolution with effect of band expansion is estimated by using Rayleigh limit as indicator. So, this result cannot be explained only by band expansion. The effect of the iterative reconstruction calculations are clearly appearing.

In the cases of sample inclined 25 degrees, and 45 degrees, the image contrast with 2-direction SWI shift is getting worse (Fig.8 (B)(b), Fig.8 (C)(b)) than the case of 10 degrees. When the profiles are seen, it is clear that it becomes impossible to resolve correct shapes. On the other hand, images obtained by 4-direction SWI shift (Fig.8 (B)(c), Fig.8 (C)(c)) resolve relatively correct shapes.

In all cases of profiles, it is seen that the value tends to emanate outside of the images. It seems that it is because of the rupture of information in the boundary.

In Fig.9, correlation coefficients between samples and super-resolution images are shown. Correlation coefficient with 4-direction SWI shift decreases until 25 degrees, and changes there to an increase until 45 degrees while correlation coefficient with 2-direction SWI shift tend to decrease until the inclination becomes 45 degrees. This result can be expected according to the direction of the band expansion (Fig.7). The correlation coefficient by 8-direction SWI shift super-resolution is shown referring. It was confirmed that more the SWI shift direction is, the higher the value of the correlation coefficient is. It seems because the influence of the discretization error is a slightly different according to angle, the behavior of the correlation coefficient in detail up and down. Correlation coefficient is about 0.86 when image obtained under the condition of Rayleigh limit, and almost all the correlation coefficients with 4-direction SWI shift are above 0.86. So, when we discuss similarity of obtained image and sample, super-resolution with 4-direction SWI shift is almost sufficient for 2-D reconstruction.

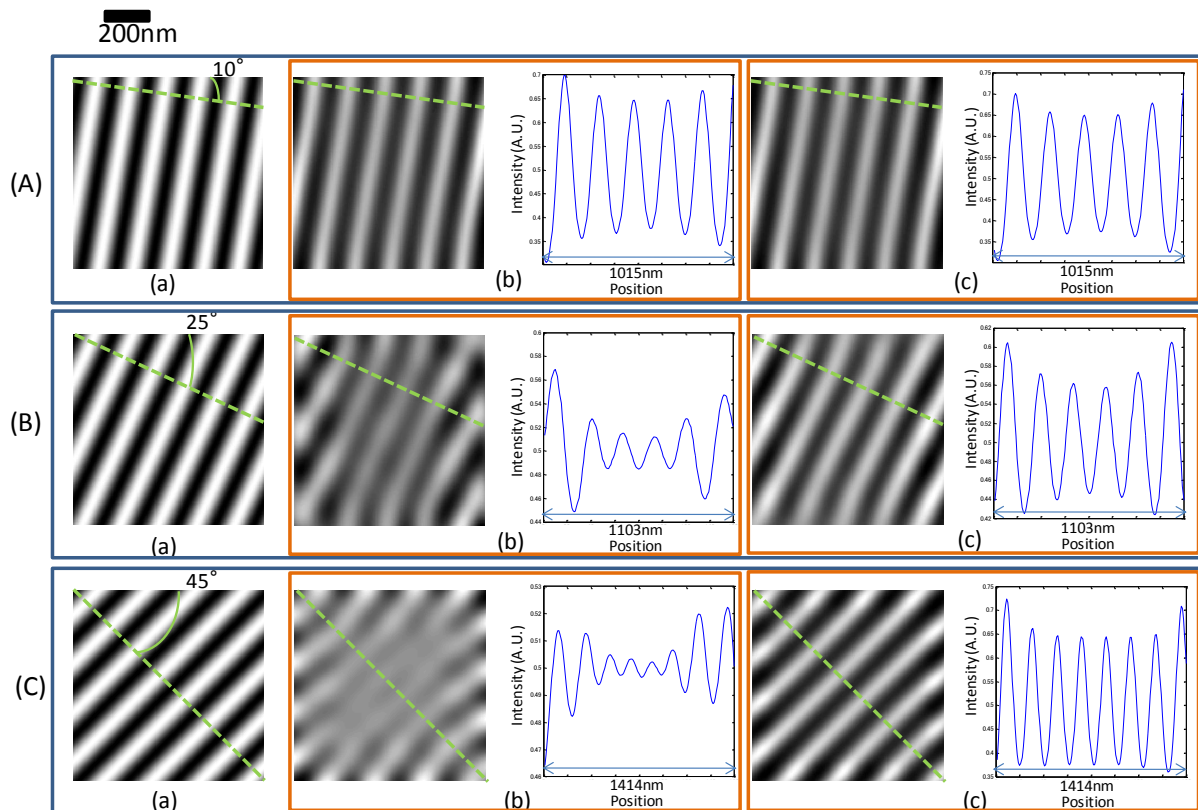


Fig. 8 Simulation for quantitative evaluation of dependency in direction (A) Inclination of sample is 10° , (B) Inclination of sample is 25° , (C) Inclination of sample is 45° (a) Samples, (b) Super-resolution images by 2-direction SWI shift (left), Profile of intensity distribution along dotted line (right), (c) Super-resolution images by 4-direction SWI shift (left), Profile of intensity distribution along dotted line (right)

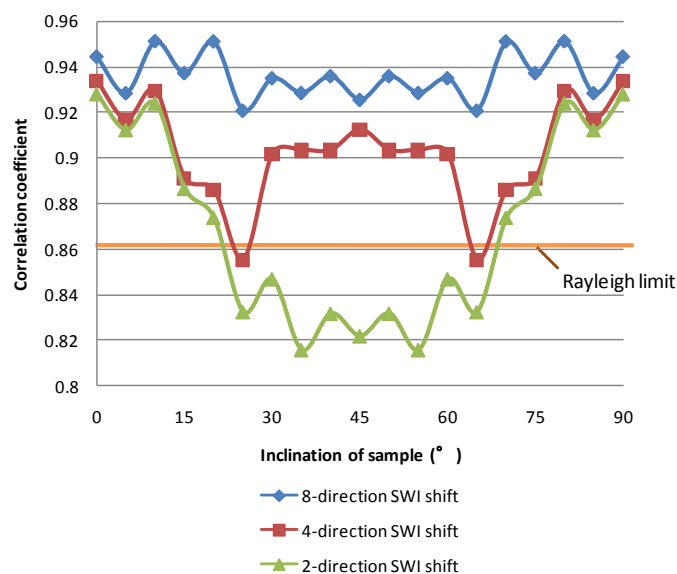


Fig. 9 Correlation coefficient between sample and super-resolution image

5. Conclusions

To realize 2-D super-resolution, the original 1-D reconstruction algorithm has been improved. As results of this improvement, saving of the computational complexity is achieved, and the 2-D reconstruction becomes possible. And it becomes possible to use the illumination which has 2-D distribution for super-resolution. And with this algorithm, 2-D super-resolution by effect of band expansion and iterative reconstruct is achieved.

To verify the resolution characteristics of the 2D super-resolution algorithm, computer simulations were carried out. By simulation with concentric circles sample, it was confirmed that the dependency by the direction was more eased by 4-direction SWI shift than 2-direction SWI shift qualitatively. To evaluate the direction dependency quantitatively, simulation with inclined periodical grating sample is carried out. The dependency by the angle of reconstructed shape was evaluated using correlation coefficient. When similarity of obtained image and sample is discussed, super-resolution with 4-direction SWI shift is almost sufficient for 2-D reconstruction. And it is confirmed that super-resolution with multidirectional SWI shift is effective to resolve 2-D structure with accurate shape.

In future work, we will improve the reconstruct accuracy of intensity by handling the rupture of information in the boundary, and verify super-resolution with multidirectional SWI shift by experimentally.

ACKNOWLEDGEMENT

This work was partially supported by Toyota Physical and Chemical Research Institute and NEDO under the Industrial Technology Research Grant Program.

The author (One of the authors (Ryota Kudo)) was supported through the Global COE Program, "Global Center of Excellence for Mechanical Systems Innovation," by the Ministry of Education, Culture, Sports, Science and Technology.

REFERENCES

1. "International Technology Roadmap for Semiconductors, Metrology (2008 update)", Semiconductor Industry Association
2. Mark A. Schulze, Martin A. Hunt, Edgar Voelkl, Joel D. Hickson, William Usry, Randall G. Smith, Robert Bryant and C. E. (Tommy)

Thomas Jr., Proc. SPIE's Advanced Microelectronic Micromanufacturing, 27-28 February 2003

3. George W. Mulholland and Thomas A. Germer, Proc. the Government Microcircuits Applications and Critical Technologies (GOMACTech) Conference, March 31 to April 3, 2003
4. Kenji Watanabe, Shunji Maeda, Tomohiro Funakoshi and Yoko Miyazaki, Hitachi Review Vol. 54, No. 1, pp22-26, 2005
5. Volker Westphal and Stefan W. Hell, PHYSICAL REVIEW LETTERS, No.143903, 2005
6. H. Nishioka, S. Takahashi, K. Takamasu, Proc. of IMEKO World Congress, 12, TC2, 2006.
7. S. Usuki, H. Nishioka, S. Takahashi, K. Takamasu, SPIE International Symposium on Optomechatronic Technologies 2005, (2005), pp60490C-1~60490C-11.
8. R. Fedosseev, Y. Belyaev, J. Frohn, A. Stemmer, Optics and Lasers in Engineering 43 (2005) 403-414
9. M. G. L. Gustafsson, Journal of Microscopy, Vol. 198, Pt 2, May 2000, pp. 82-87.